Since January 2020 Elsevier has created a COVID-19 resource centre with free information in English and Mandarin on the novel coronavirus COVID-19. The COVID-19 resource centre is hosted on Elsevier Connect, the company's public news and information website.

Virology 407 (2010) 185–195

Contents lists available at ScienceDirect

Virology

journal homepage: www.elsevier.com/locate/yviro

Fragmentation of the Golgi apparatus provides replication membranes for human rhinovirus 1A

Claire A. Quiner [1], William T. Jackson *

Department of Microbiology and Molecular Genetics and Center for Infectious Disease Research, Medical College of Wisconsin, Milwaukee, WI, USA

ARTICLE INFO

Article history:
Received 18 May 2010
Returned to author for revision 11 June 2010
Accepted 12 August 2010
Available online 9 September 2010

Keywords:
Rhinovirus
Picornavirus
Golgi fragmentation
Replication membranes

ABSTRACT

All viruses with a positive-stranded RNA genome replicate their genomic RNA in association with membranes from the host cell. Here we demonstrate a novel organelle source of replication membranes for human rhinovirus 1A (HRV-1A). HRV-1A infection induces fragmentation of the Golgi apparatus, and Golgi membranes are rearranged into vesicles of approximately 250–500 nm diameter. The newly distributed Golgi membranes co-localize with viral RNA replication templates, strongly suggesting that the observed vesicles are the sites of viral RNA replication. Expression of the HRV-1A 3A protein induces alterations in the Golgi staining pattern similar to those seen during viral infection, and expressed 3A localizes to the Golgi-derived membranes. Taken together, these data show that in HRV-1A infection, the 3A protein plays a role in fragmenting the Golgi complex and generating vesicles that are used as the site of viral RNA replication.

Introduction

All positive-strand RNA viruses studied to date replicate their RNA in association with cellular membranes (Miller and Krijnse-Locker, 2008). The origin of these membranes varies widely among viruses. For example, the alphanodavirus Flock House Virus replicates on invaginations of the mitochondrial membrane (Miller et al., 2001). SARS virus, a coronavirus, replicates on a reticulovesicular network derived from the endoplasmic reticulum (ER) (Knoops et al., 2008). The flavivirus Hepatitis C Virus performs RNA replication on a "membranous web" thought to be derived from ER membranes and lipid droplets (Tang and Grise, 2009). Semliki Forest Virus, an alphavirus, replicates on cytopathic vesicles thought to be derived from endosomes and lysosomes (Salonen et al., 2003; Spuul et al., 2007). These examples, while by no means comprehensive, serve to demonstrate the large variation in the origin of viral replication membranes.

The origin of replication vesicles for the type picornavirus, poliovirus, has been controversial. Previously, we demonstrated that poliovirus induces autophagosome-like double-membraned vesicles, and that these vesicles are the sites of RNA replication (Jackson et al., 2005). Other viruses use the autophagic machinery to enhance viral replication, including Dengue Fever Virus, Hepatitis C Virus, Coxsackie B3 Virus, and the rhinoviruses HRV-2 and HRV-14 (Ait-Goughoulte et al., 2008; Dreux et al., 2009; Jackson et al., 2005; Khakpoor et al., 2009; Lee et al., 2008; Sir et al., 2008; Wong et al., 2008). Not all viruses use the autophagy machinery in the same way. For example, Hepatitis C virus replication membranes do not look like conventional autophagosomes, although the autophagosomal machinery is important for initiating viral replication (Dreux et al., 2009; Moradpour et al., 2003).

A second hypothesis for generation of poliovirus replication vesicles involves diversion of anterograde secretory vesicles coated with proteins of the COPII complex (Rust et al., 2001). Markers for COPII co-localize with the viral replication protein 2B on vesicles that appear to bud from the ER. However, several lines of evidence argue against the COPII hypothesis, including the sensitivity of poliovirus to Brefeldin A, which inhibits COPI but not COPII vesicle formation (Gazina et al., 2002; Maynell et al., 1992). In addition, poliovirus replication is not inhibited by expression of a dominant-negative allele of the COPII protein Sar1, which blocks anterograde transport (Taylor, 2007). Nonetheless, the COPII hypothesis may be compatible with the autophagy hypothesis, as COPII components have been shown to be important for autophagy in *Saccharomyces cerevisiae* (Hamasaki et al., 2003; Ishihara et al., 2001).

In previous work we demonstrated that two rhinoviruses, HRV-2 and HRV-14, induce autophagic vesicles resembling those observed during poliovirus infections (Jackson et al., 2005). The HRV-2 result has been controversial, with a report showing that under different experimental conditions, HRV2 will not induce or respond to autophagic induction (Brabec-Zaruba et al., 2007). We plan to address this controversy in a separate study. However, the enormous genetic diversity of rhinoviruses makes it likely that we will find diverse membrane origins within these closely related viruses.

* Corresponding author. Fax: +1 414 955 6535.
E-mail address: wjackson@mcw.edu (W.T. Jackson).
[1] Present address: School of Public Health, University of California, Berkeley, CA 94720, USA.

0042-6822/$ – see front matter © 2010 Elsevier Inc. All rights reserved.
doi:10.1016/j.virol.2010.08.012

Rhinoviruses are, like poliovirus, a part of the *Enterovirus* genus, and represent a large and diverse collection of at least 138 viruses, most of which have only recently been sequenced (Palmenberg et al., 2009). Human rhinoviruses are classified into major group viruses, which use the ICAM-1 receptor for cell entry, and minor group viruses, which enter cells by binding the low-density lipoprotein receptor (Uncapher et al., 1991). They have been further classified into HRV-A, HRV-B, and HRV-C groupings, the first two of which were originally determined by their resistance to distinct classes of antiviral compounds (Andries et al., 1990). The HRV-C group was more recently identified using viral genomic array technology, and all three groupings have been verified and refined by modern sequence analysis (Kistler et al., 2007; Palmenberg et al., 2009).

Complete cDNA clones are available for producing several rhinoviruses, including the HRV-1A, HRV-2, and HRV-14 strains (Callahan et al., 1985; Duechler et al., 1989). The availability of these clones allows production of isogenic stocks of virus; otherwise, repeated virus passaging allows genomic drift to occur due to the low fidelity of the RNA-dependent RNA polymerase (Wells et al., 2001). Close study of such a large and closely related group of viruses will reveal both differences and commonalities in generating replication membranes.

Here we investigate the origin of replication membranes for one of the cloned rhinoviruses, HRV-1A, a minor group, HRV-A type virus. We show that, unlike poliovirus, HRV-1A does not induce or respond to the autophagic pathway. In addition, we provide evidence that during HRV-1A infection, the Golgi is fragmented into vesicles that appear to be used as a substrate for viral RNA replication. Finally, we show that expression of the HRV-1A 3A protein induces changes in Golgi staining reminiscent of the changes during HRV-1A infection, and that the 3A protein co-localizes with the fragmented Golgi signal. These data, taken together, indicate that HRV-1A uses the Golgi apparatus as a source of RNA replication vesicles.

Results

Rhinovirus and autophagy

In previous work, we showed that poliovirus and two strains of rhinovirus induce the formation of autophagosome-like vesicles during infection, the cytoplasmic faces of which are used as a substrate for viral RNA replication (Jackson et al., 2005). Here we extend our studies on viruses and autophagy to another cloned rhinovirus strain, HRV-1A. Background levels of autophagy vary from cell line to cell line, so for these assays we used 293T human embryonic kidney cells, which have a low background level of autophagy (Tanida et al., 2005). The best marker for autophagosome formation is the microtubule-associated light chain 3 (MAP-LC3, also known as hATG8 or LC3) protein, which is required for generating nascent autophagic membranes (Klionsky et al., 2008). As autophagic signaling is induced, cellular pools of LC3 become lipidated and associated with autophagosome membranes. Cytoplasmic GFP-LC3 indicates low levels of autophagy, while punctate LC3 signal indicates increased membrane association of LC3 on autophagosomes (Klionsky et al., 2008).

To examine induction of autophagosomes, 293T cells were transfected with a plasmid expressing a GFP-LC3 fusion protein (Jackson et al., 2005). Two days after transfection, cells were infected with virus at an MOI of 50, mock infected, or treated with rapamycin to induce autophagy. For each condition, three replicate samples of at least 100 transfected cells each were counted under double-blinded conditions. LC3 signal was scored as punctate or non-punctate. Some representative images are depicted in Fig. 1A. Double-blinded quantitation of these images, in which cells were scored as punctate or non-punctate, is shown in Fig. 1B. The mock-infected cells demonstrated low, intrinsic levels of LC3 puncta, and HRV-1A-infected cells have equivalent levels. However, in PV-infected and rapamycin-treated cells, approximately half of the population displayed LC3 puncta, an increase in puncta formation similar to that seen previously for PV (Taylor et al., 2009). In addition, we have also found that HRV-1A yield does not vary upon stimulation or inhibition of autophagy (data not shown). These data indicate that the autophagic pathway is not induced or subverted by HRV-1A infection.

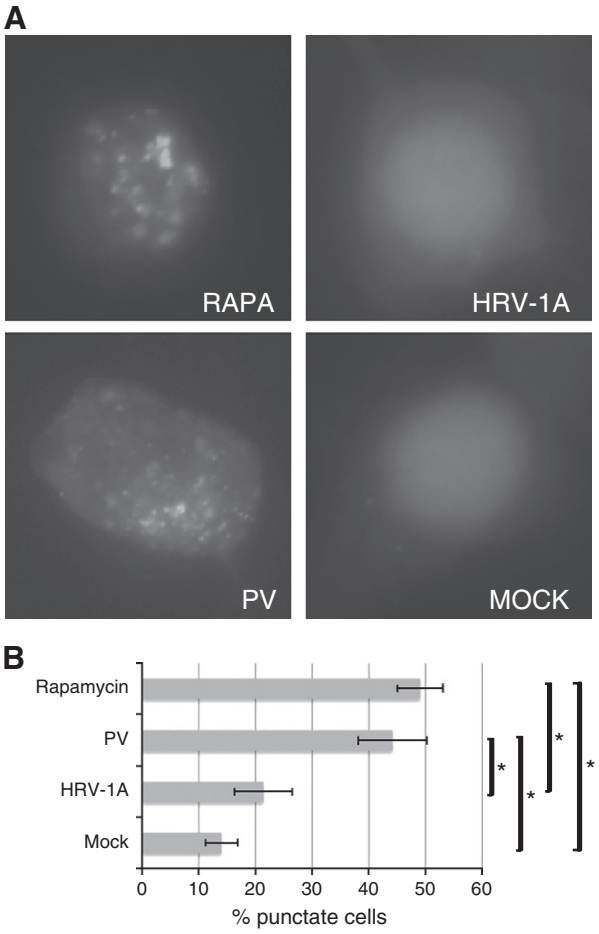

Fig. 1. Poliovirus, HRV-1A, and autophagy. (A) Representative images of punctate and non-punctate GFP-LC3 localization from infected, mock-infected, and rapamycin-treated cells. (B) Quantitation of autophagic induction. Cells transfected with GFP-LC3 were infected at an MOI of 50, treated with rapamycin, or mock treated for 6 h, then fixed. A minimum of 100 cells were scored for punctate or cytoplasmic LC3 staining. The percentage of punctate cells is shown. Asterisks indicate comparison of two conditions by Student's *t*-test in which $p<0.05$.

Organelle staining in HRV-1A-infected cells

Since we did not observe autophagic induction during HRV-1A infection, we wanted to observe cellular organelle markers for potential changes during HRV-1A infection. WI-38 embryonic lung fibroblasts have an ideal morphology for immunofluorescence analysis and are one of the few cell lines that can be infected by all rhinoviruses (Dolan et al., 1968). A single-cycle poliovirus or rhinovirus infection in WI-38 cells proceeds for 48–56 h before the cytopathic effect is observed (Fenters et al., 1967) a time course of infection that we have confirmed. Therefore, we fixed cells 24 h post-infection to visualize morphological changes at the mid-point of the viral life cycle. Virus stocks were assessed by $TCID_{50}$ assay in WI-38 cells, and infections were performed at matched $TCID_{50}$.

First we tested the endoplasmic reticulum (ER) (Fig. 2, top). We stained infected cells with Protein Disulfide Isomerase (PDI) to observe the relative morphology of the ER. The characteristic lace-like pattern of the ER can be seen, with denser regions near the nucleus. This ER pattern, seen in mock-infected cells, is

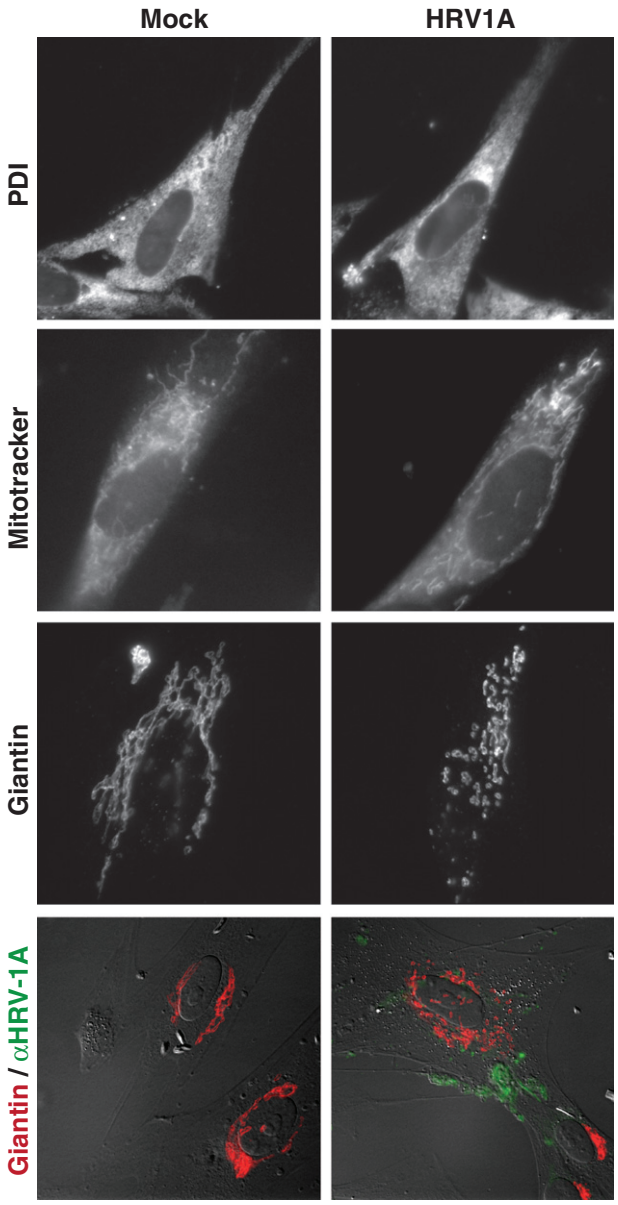

Fig. 2. Organelle marker staining of infected cells. WI-38 cells were mock infected or infected with HRV-1A at four logs above the $TCID_{50}$ for 24 h. Cells were fixed in formaldehyde and stained with antibodies to Protein Disulphide Isomerase (PDI). At 24 h post infection, cells were stained with MitoTracker for 45 min before fixation. Formaldehyde-fixed cells were stained for Giantin. Bottom row: cells were stained for Giantin (red) and co-stained for HRV-1A capsid antibody (green), and fluorescent signal overlaid with DIC images. Representative cells from each experiment were imaged.

indistinguishable from that observed in infected cells. Next, we stained infected cells with the live stain MitoTracker to observe potential changes in the distribution or structure of the mitochondria. We observe a typical reticulotubular pattern of mitochondrial staining, and there were no significant changes in the staining pattern between infected and uninfected cells (Fig. 2, second row).

Next we analyzed the Golgi apparatus. Infected and fixed cells were stained for the Golgi cisternae marker Giantin (Fig. 2). The continuous cisternae of the Golgi are clearly visible in a perianuclear region of mock-infected cells. This typical pattern was not visible in the majority of HRV-1A-infected cells. Instead, the Giantin staining in these cells is disjointed and fragmented, with puncta and small oval-shaped structures spread throughout the cell. To confirm that this effect was related to infection, we co-stained for Giantin (red) and an antibody to detect the HRV-1A capsid (green). While capsid protein is not present in replication complexes, the presence of capsid in a cell indicates viral entry. Mock-infected cells did not stain with capsid antibody, and the Golgi appeared normal (Fig. 2, bottom row). All cells in the infected population stained with capsid antibody, and in these cells Giantin signal was abnormal, often appearing as punctae throughout the cytoplasm. These fluorescent images were overlaid on DIC images of the cells to show the perinuclear location of the Golgi signal.

To better observe the development of these unusual patterns of Giantin staining, we performed a time course of infection (Fig. 3). At 6 h post-infection with HRV-1A, Golgi staining appears only slightly more compacted than those in matched PV or mock infections. By 12 h post-infection, the Golgi complex is more fragmented and spread throughout the infected cell. This pattern continues until 24 h, when the Giantin signal is distributed around the cell and fragmented into puncta and small oval structures, with few reticular networks visible. At 24 h post-infection with PV, we still identify a complex network of continuous Golgi staining comparable to uninfected cells. These data indicate that HRV-1A infection induces significant morphological changes in the Golgi complex.

Since airway epithelial cells are the primary sites of HRV infection *in vivo*, we wanted to determine if Golgi staining patterns were altered in an airway epithelial-derived cell line (Lopez-Souza et al., 2009). BEAS-2B lung epithelial cells were infected with HRV-1A (Fig. 4). At 24 h and 72 h post-infection, cells were fixed and stained for both Giantin and a second Golgi marker, GM130, to ensure that the redistribution of signal was not specific to Giantin. At 24 h.p.i., we observed a redistribution of both Golgi markers. GM130 and Giantin are found throughout the cytoplasm of uninfected cells but are restricted to a small juxtanuclear region of HRV-1A-infected BEAS-2B cells. This staining pattern is identical at 48 h.p.i. (data not shown). At 72 h.p.i. it is difficult to identify Golgi markers in any organized pattern, and staining is punctate and spread throughout the cytoplasm (Fig. 4). HRV-1A-infected BEAS-2B cells begin to round up and lyse between 72 h and 84 h post-infection. At each observed time point, both GM130 and Giantin re-localized, indicating that the redistribution likely represents Golgi membrane redistribution, rather than movement of a single marker to a different cellular location.

Sites of HRV-1A genome replication

Since the Giantin staining pattern was altered during HRV-1A infection, we wanted to determine if the site of viral RNA replication followed a similar pattern. To detect the sites of active RNA replication, we synthesized fluorescent-labeled positive-sense RNA probes *in vitro*. These probes hybridize to the negative-sense RNA intermediate that is synthesized as a template for genomic synthesis (Teterina et al., 2001). Our attempts at co-staining with antibody and riboprobes destroyed RNA signal, presumably due to RNAses in the antibody preparations, so the Giantin antibody was not used for this experiment. Instead, WI-38 cells were first treated with the "Golgi Organelle Lights RFP" reagent (Invitrogen), which allows visualization of the Golgi stacks (Tan et al., 2009). This reagent expresses RFP fused to the Golgi resident protein N-acetylgalactosaminyltransferase-2.

48 h after treatment with Organelle Lights, cells were infected with HRV-1A for 24 h (Fig. 5A–F) or mock infected (G–I). Samples were fixed and RNA probes were hybridized to cells *in situ*. Cells were then imaged for the Golgi marker and either HRV-1A RNA (B, H) or poliovirus RNA (E). Mock-infected cells (G–I) display intact Golgi with clearly defined continuous patterns of staining, and background levels of RNA hybridization. HRV-1A-infected cells (A–F) show a fragmented juxtanuclear Organelle Lights Golgi signal. This signal co-localizes with a positive-sense HRV-1A genomic RNA probe (B) but not with a probe specific to poliovirus genomic RNA (E), indicating that the signal is specific. The majority of negative-strand templates are involved in RNA replication (Teterina et al., 2001). Therefore, these

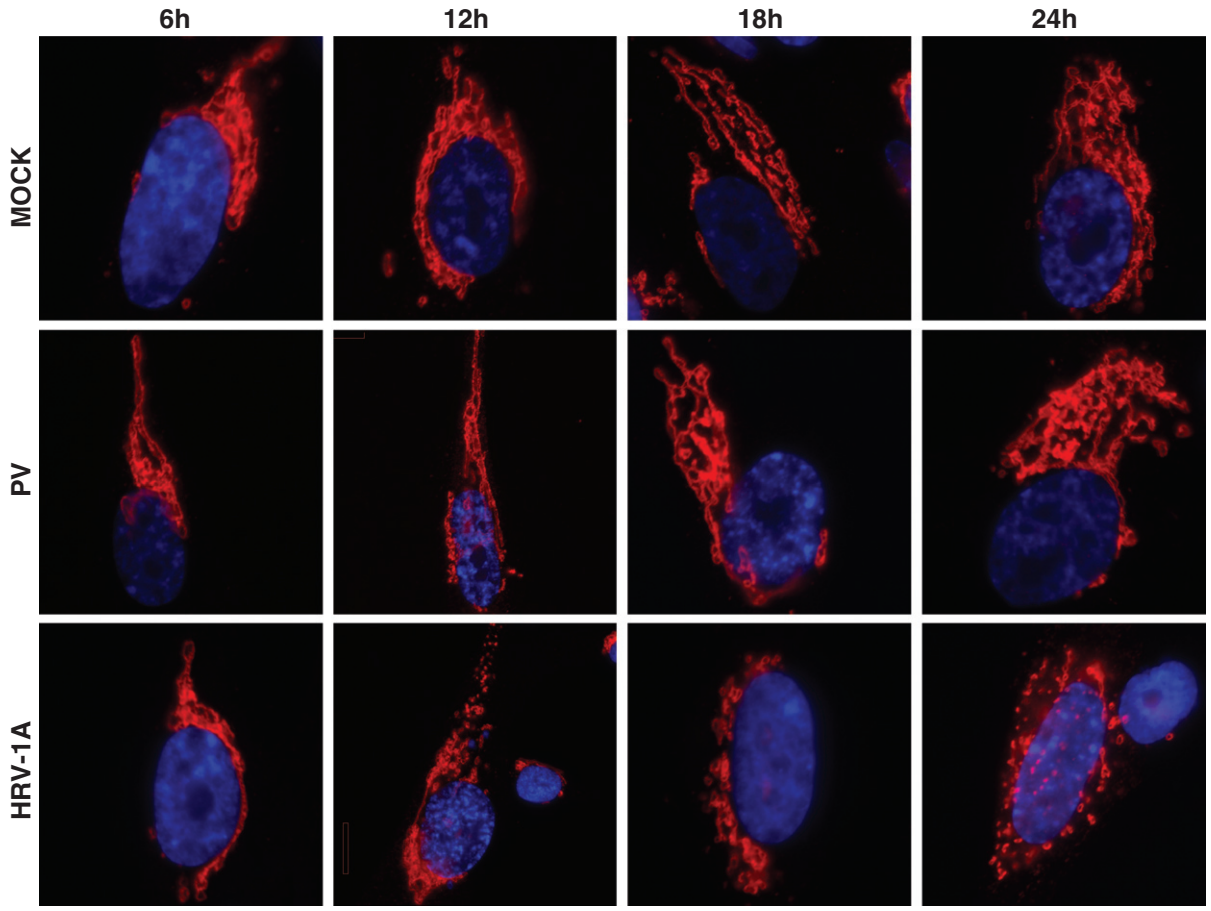

Fig. 3. Time course of Giantin staining during infection. WI-38 cells were infected at four logs above the $TCID_{50}$ for the indicated times with PV, HRV-1A, or mock infected. Cells were then fixed and stained for Giantin as in Fig. 2. Cells were additionally stained for DAPI to visualize nuclei. Representative cells from each time point were imaged.

data indicate that altered Golgi morphologies likely represent active sites of HRV-1A genome replication.

Electron microscopy of HRV-1A-infected cells

To further understand these cellular changes at the ultrastructural level, we performed electron microscopy on mock-infected or HRV-1A-infected WI-38 cells (Fig. 6). Infection was confirmed by removing a portion of the culture before fixation and observing synchronous cell lysis at 48–54 h.p.i. In mock-infected cells, we are able to identify ordered stacks of membrane we identified as Golgi (closed white arrowheads). The ultrastructure of cells infected with HRV-1A for 24 h is distinct from that of uninfected cells. Elongated stacks of membranes are rarely seen, and when they are, they are disorganized (open white arrowheads). In HRV-1A infected cells, these stacks are not ordered, while similar stacks visible in mock-infected cells are regularly spaced and ordered. HRV-1A-infected cells also displayed larger, dark-staining, ovoid vesicles of approximately 250–500 nM in diameter. These vesicles, whose contents appear more electron dense than the surrounding cytoplasm, can be seen throughout the cytoplasm of infected cells. We do not observe structures in HRV-1A-infected cells that have the size or characteristics of autophagosomes or autolysosomes. Based on these studies, HRV-1A appears to uniquely alter cellular morphology, resulting in small vesicles distinct from those observed in autophagic or PV-infected cells (Jackson et al., 2005).

In order to analyze the redistribution of Giantin signal during HRV-1A infection, we performed immuno-EM analysis using our Giantin antibody and gold-labeled secondary (Fig. 7). Golgi membranes are more difficult to observe in our immuno-EM preparations due to differences in the fixation and staining protocol. However, we were able to detect Giantin staining in linear patterns, on apparent membranes, in the cytosol of mock-infected cells (closed arrowheads). In contrast, HRV-1A infected cells showed a pattern of Giantin staining near large vesicles (open arrowheads). The Giantin-staining vesicles have light-staining contents in these images, possibly because the vesicular contents were extracted as a result of the immuno-EM preparation. Upon observation of over 100 cells, we did not find linear, Golgi-like patterns of Giantin staining in HRV-1A infected cells. Therefore, the vesicles we observe are likely to represent fragmented Golgi membranes.

Expression of HRV-1A 3A protein

The 3A nonstructural protein from poliovirus is a 10kD transmembrane protein required for RNA replication (Berstein and Baltimore, 1988; Choe and Kirkegaard, 2004; Teterina et al., 2003). During PV infection, 3A is found in the replication membranes. However, when expressed in isolation, PV 3A localizes to the ER (Suhy et al., 2000). We were interested in determining the effect of HRV-1A 3A protein expression as well as its localization within cells. Lentivirus-based constructs, which express both the protein of interest and GFP, were generated with two versions of HRV-1A 3A. One has an HA antigenic tag on the C-terminus, and the other is untagged. WI-38 cells were infected and observed until GFP expression was visible (A,E,I) then fixed and stained for Giantin (B,F,J) and HA (C,G,K). Production of 3A-expressing lentivirus was not robust; in order to detect expression, we needed to concentrate lentivirus by centrifugation. Even after concentration, not every cell in our target cultures received lentivirus. We presume that the low production of lentivirus is due to the known toxicity of the 3A protein, since we did not have this problem with

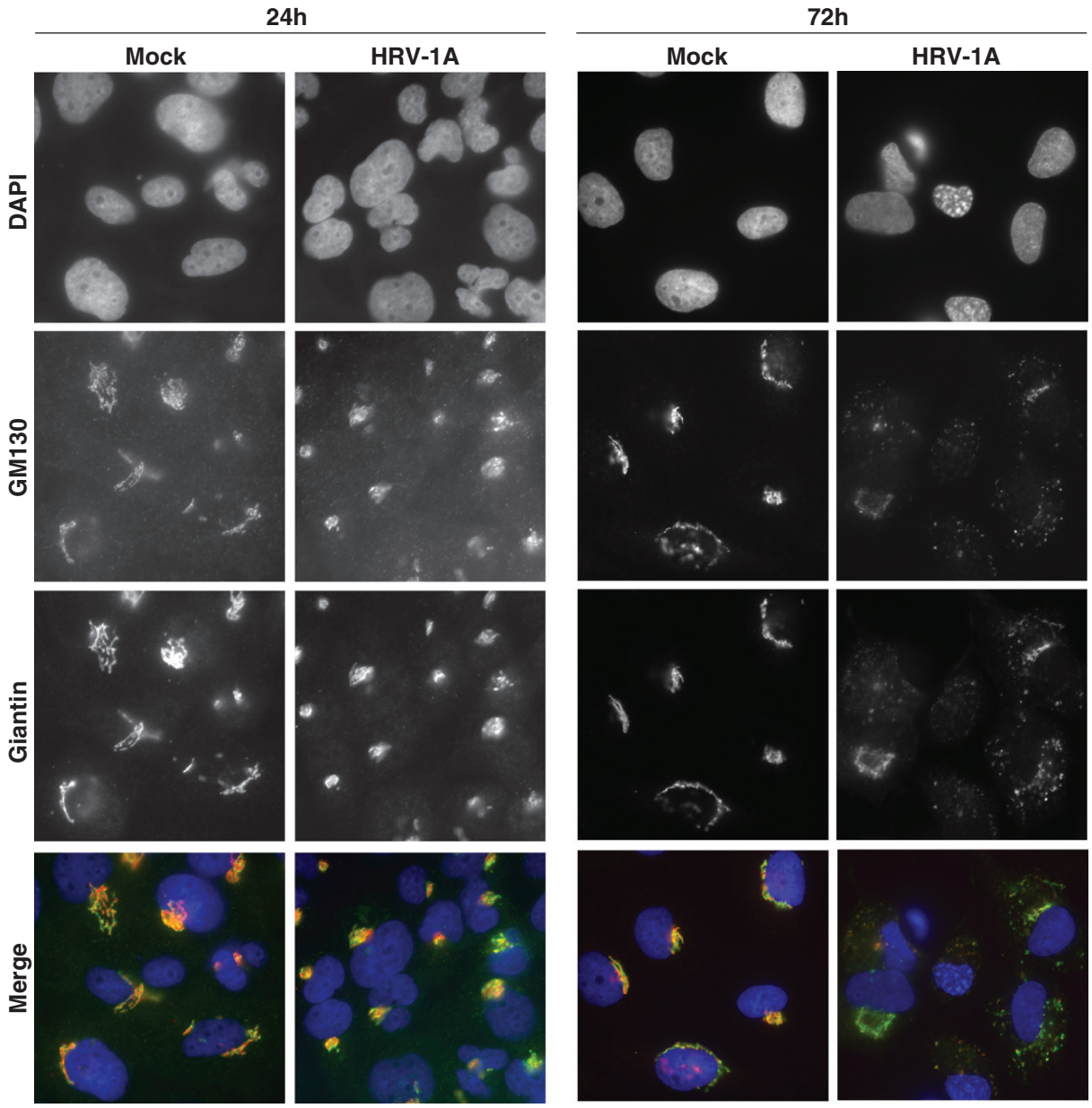

Fig. 4. Golgi redistribution in HRV1A-infected lung epithelial cells. BEAS-2B cells were infected at four logs above the $TCID_{50}$, then fixed at 24 h.p.i. or 72 h.p.i. Cells were stained for Giantin, GM130, and DAPI. Individual images are shown, and merged, bottom row.

lentiviruses that did not express 3A (Lama et al., 1992). However, this allows for internal controls in each experiment. We have provided fields that contain cells with and without lentivirus expression for direct comparison (Fig. 8).

A vector-carrying lentivirus, which expresses GFP but no 3A protein, displays normal Golgi morphology with continuous cisternae clearly visible (A–D) indicating that the lentivirus system itself does not alter Golgi staining. We were able to detect the HA-tagged form of 3A in lentivirus vector-expressing cells, which can further be identified by the presence of GFP (E–H). We found that in 3A-HA expressing cells, the pattern of Golgi staining changed, condensing to a juxtanuclear region of the cell with distinct cisternae no longer visible. Cells in the same field not receiving lentivirus (closed arrowheads) display a normal pattern of Giantin staining. The pattern of 3A-HA staining overlaps with Giantin staining, indicating that the tagged version of HRV-1A 3A localizes to these altered Golgi membranes.

To determine if the HA antigenic tag altered the function of the 3A protein, we expressed an untagged version of the protein (Fig. 8, panels I–L). In GFP-positive cells (open arrowhead) the Giantin signal is no longer in continuous lines but in diffuse puncta. While we do not have the reagents to determine where the untagged 3A protein localizes, this experiment does demonstrate a dramatic effect of 3A expression on Golgi morphology. Taken together, the experiments in Fig. 8 indicate that HRV-1A 3A is sufficient to induce changes in Golgi morphology. In addition, the 3A-HA protein localizes to the altered Golgi membranes.

Discussion

Our work here demonstrates that HRV-1A, like all positive-stranded RNA viruses investigated to date, replicates its RNA in association with cellular membranes. The novel finding about HRV-1A genomic RNA replication is the source of the replication membranes. A redistribution of the Golgi marker Giantin takes place during infection, resulting in a condensation of the signal into a perinuclear region, followed by puncta scattered throughout the cell. Negative-

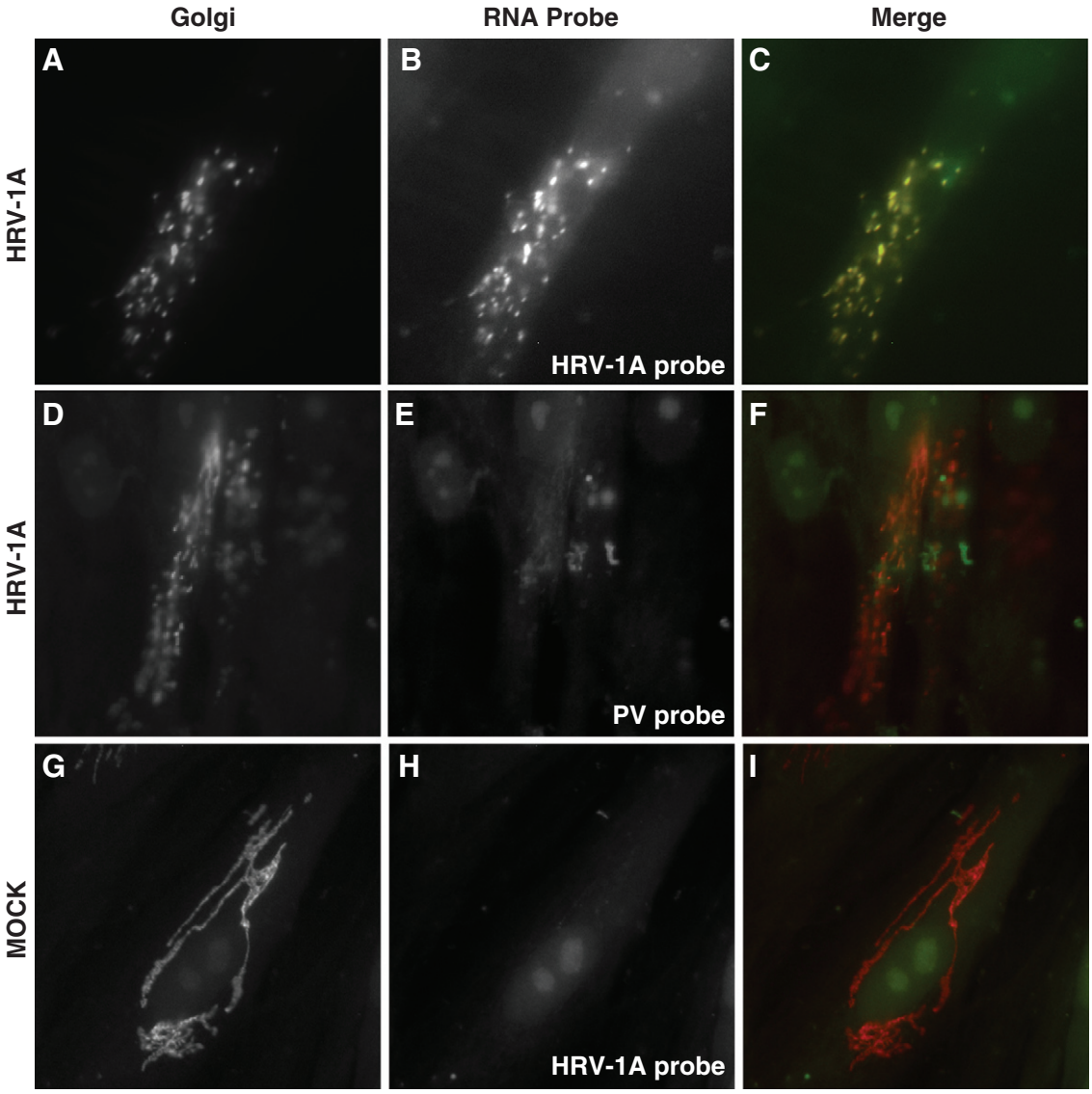

Fig. 5. Localization of Golgi and HRV-1A negative-strand RNA. Cells were treated for 48 h with Organelle Lights Red Golgi (A,D,G) then infected with HRV-1A (A–F) or mock-infected (G–I) for 24 h. After fixation, a positive sense Alexa Fluor 488-labeled HRV-1A RNA probe (B, H) or poliovirus RNA probe (E) was hybridized to the cells to detect negative-stranded replication intermediates. Cells were then processed for imaging, and Golgi and RNA signals were merged (C, F, I).

stranded viral RNA, an intermediate in viral replication, also co-localizes with a Golgi marker, indicating that viral RNA replication occurs in association with fragmented Golgi membranes.

Our electron microscopy images (Fig. 6) of HRV-1A infected cells reveals the presence of electron-dense vesicles of approximately 250–500 nm in diameter. These vesicles, which appear to be multilamellar, are not visible in mock-infected WI-38 cells. In our observations of at least 100 cells, there is a correlation between the appearance of the electron-dense vesicles and the disorganization of Golgi-like stacks in infected cells, although it is difficult to identify a "Golgi-like stack" given the disorganized nature of membranes in HRV-1A infected cells (Fig. 5). Our immunostained EM images (Fig. 7) show Giantin staining on vesicles of approximately 500 nm as well. Although the Giantin-stained vesicles are not electron dense, we believe that extraction of vesicle contents may be the result of preparation for immunostaining. Therefore, they are likely the same 500-nm vesicles seen in conventional EM.

The 500-nm vesicles coincide with the only significant Giantin staining in HRV-1A infected cells, so we believe they represent the Giantin-stained puncta seen by immunofluorescence microscopy in Figs. 2–4. Since a Golgi marker also co-localizes with negative-strand viral RNA (Fig. 5) we believe that the electron-dense vesicles in Fig. 6 likely represent the sites of viral replication. Our model, unique to HRV-1A of viruses studied, is that the Golgi fragments into vesicles that serve as substrates for viral replication. It has been reported that poliovirus causes fragmentation of the Golgi during late infection, but that these membranes are not the sites of viral replication. (Beske et al., 2007). At 24 h of a PV infection of WI-38 cells, we do not observe Golgi fragmentation. Foot-and-mouth disease virus (FMDV) forms replication sites near the Golgi apparatus, but Golgi markers are specifically excluded from the replication membranes (Knox et al., 2005). Therefore, this study marks the first demonstration, to our knowledge, that the Golgi provides replication membranes to a positive-strand RNA virus.

For insight into the possible mechanisms by which HRV-1A hijacks Golgi membranes for replication, we have considered some known pathways of Golgi fragmentation. For example, Brefeldin A, which targets the ARF1 GTPase, can induce Golgi fragmentation. The effect of Brefeldin A on the Golgi is morphologically similar to that of HRV-1A infection (Hidalgo et al., 1992; Radulescu et al., 2007). PV replication is extremely sensitive to Brefeldin A treatment, suggesting that ARF1 function is important to the

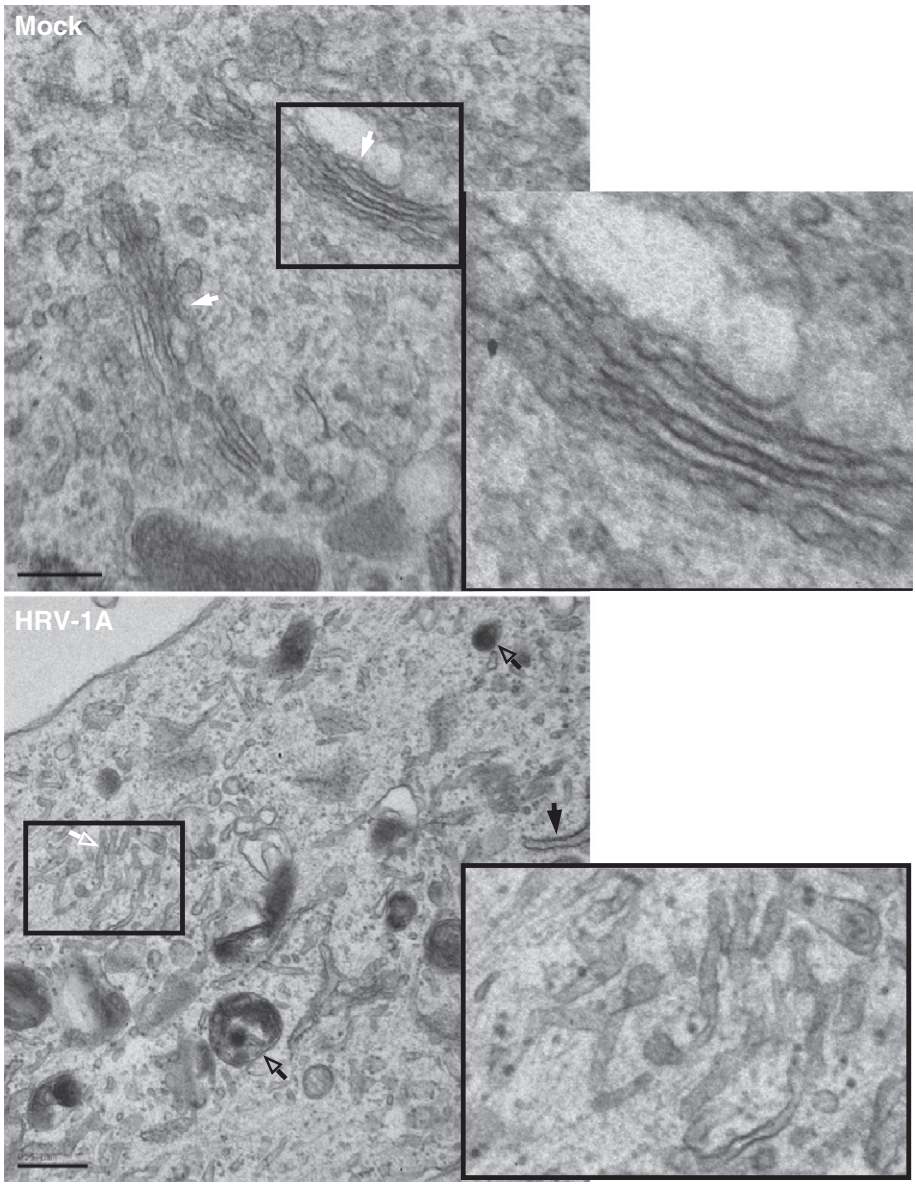

Fig. 6. Electron Microscopy of Infected WI-38 lung fibroblasts. Cells were mock infected or infected with HRV-1A at four logs above the $TCID_{50}$ for 24 h. Organized Golgi stacks can be seen in Mock-infected cells (closed white arrowheads) but not HRV-1A-infected cells, which instead display disorganized areas of elongated membrane (open white arrowheads). N = Nucleus. Rough ER can be seen as distinct structures (closed black arrowheads). Dark-staining vesicles approximately 250–500 nM across are observed in HRV-1A infected cells (open black arrowheads). Note that there is no gold-particle labeling in these images; the small particles visible are likely to be virions. All bars = 0.5 μM.

virus (Kirkegaard, 1992). Other picornaviruses vary in their sensitivity to Brefeldin A (Gazina et al., 2002). ARF1 plays key roles in membrane trafficking and has been implicated in Golgi fragmentation during both mitosis and nocodazole treatment (Bui et al., 2009; Tang et al., 2008). Guanine exchange factors (GEFs) for ARF1 are recruited to poliovirus membranes by two different poliovirus proteins (Belov et al., 2007). GBF1, an ARF1 GEF recruited by poliovirus 3A, is also recruited by the 3A protein of another picornavirus, Coxsackievirus B3 (Wessels et al., 2006). However, the 3A proteins from HRV-2 and HRV-14 do not recruit GBF1 to replication membranes, indicating that this is not universal among picornaviruses (Wessels et al., 2006). We have found that HRV-1A replication is extremely sensitive to Brefeldin A1. (Data not shown). These data indicate that the importance of ARF1 in picornavirus replication is independent of the organelle source of the viral replication membrane.

The picornavirus 3A transmembrane protein is involved in organelle rearrangements to generate replication membranes. In this study we show that HRV-1A 3A can be expressed in isolation to induce rearrangements of a Golgi marker within cells. In addition, an epitope-tagged version co-localizes with the Golgi signal. These data, along with our FISH data (Fig. 5), lead us to the model that HRV-1A replicates its RNA in association with Golgi-derived vesicles, and that the 3A protein plays a role in generating these replication membranes. The effect of picornavirus 3A proteins on the Golgi is distinct depending on the viral origin of the protein. When expressed in isolation, poliovirus 3A localizes to the ER and induces swelling and distension of that organelle, but no effects on the Golgi complex were reported (Doedens et al., 1997; Suhy et al., 2000). Another group demonstrated that expression of poliovirus 3A is capable of dispersing the Golgi. The same study showed that myc-tagged 3A proteins from Coxsackievirus B3, HRV-2, and HRV-14 localize to the Golgi complex when expressed in cells (Wessels et al., 2006). Coxsackievirus B3 3A protein can fragment the Golgi as well (Cornell et al., 2006).

We believe HRV-1A replication membranes derive from the Golgi apparatus through an unknown mechanism. In contrast, PV replication

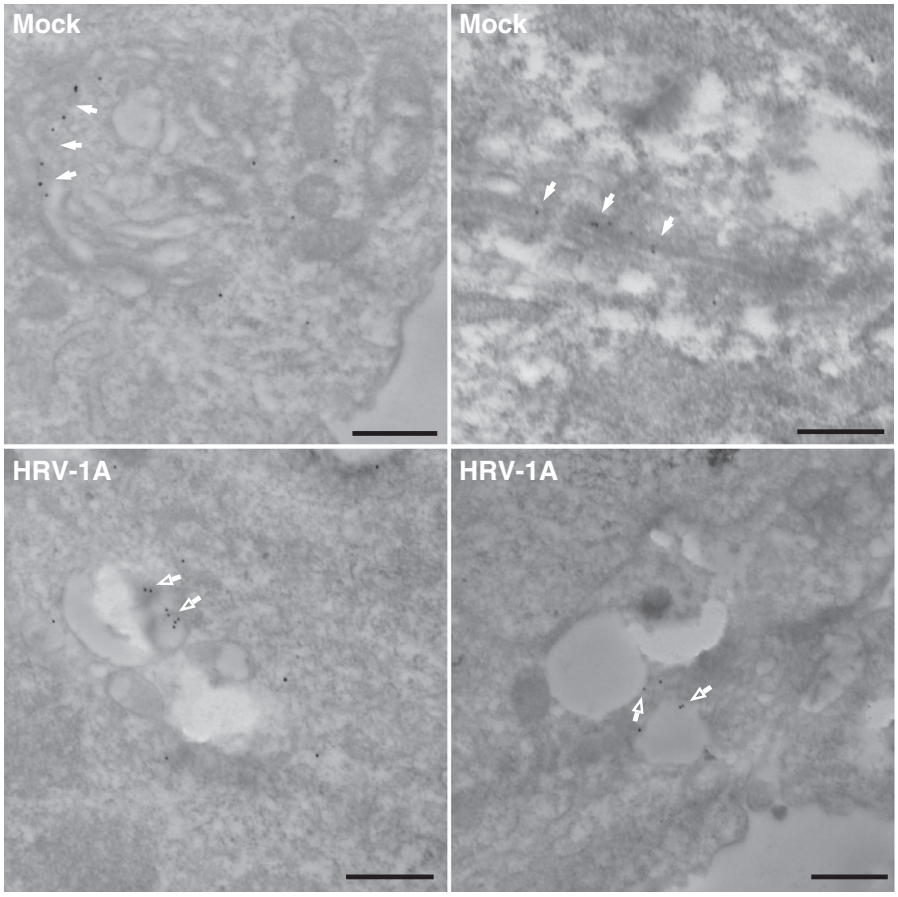

Fig. 7. Immunostained electron microscopy of infected WI-38 lung fibroblasts. Samples were processed for immuno-EM using Giantin polyclonal antibody and gold-labeled secondary antibody. Giantin staining can be seen in linear patterns in Mock-infected cells (closed arrowheads). For HRV-1A-infected cells, Giantin staining coincides with large vesicles (open arrowheads) of approximately 500 nM in diameter. All bars = 0.5 μM.

membranes likely derive from the ER, either through the autophagosome or COPII pathways, or possibly both. When the 3A proteins of PV and HRV-1A are expressed in isolation, each localizes to the organelle hypothesized to be the source of replication membranes: the ER for PV, and the Golgi for HRV-1A. This may be a mechanistic insight into a picornavirus strategy for generating vesicles. The presence of the 3A protein, possibly very early during infection, could mark an organelle as the source of membranes for viral RNA replication.

In summary, we believe the marked difference in membrane phenotype between genotypically similar viruses will lead to insights regarding the mechanism of membrane generation by RNA viruses. If 3A is a common marker of organelles destined to become viral replication membranes, then the differences between viral 3A proteins can reveal novel localization signals and provide an understanding of membrane rearrangements.

Materials and methods

Cells, virus, and plasmids

WI-38, 293T, and H1-HeLa cells were obtained from the American Type Culture Collection (ATCC, Manassas, Virginia, United States) and grown essentially according to ATCC protocols. WI-38 cells were grown in Minimal Essential Medium (MEM) supplemented with 10% fetal bovine serum and sodium pyruvate. 293T cells were grown in High Glucose D-MEM supplemented with 5% calf serum and 5% fetal bovine serum. H1-HeLa cells were grown in MEM supplemented with 10% calf serum. BEAS-2B cells were a gift from Charles Myers (Department of Pharmacology and Toxicology, Medical College of Wisconsin) and were grown in D-MEM supplemented with 10% fetal bovine serum and 10% LHC-9 complete medium (Invitrogen). All cell lines were maintained at 37 °C with 5% CO_2 in the presence of Penicillin and Streptomycin. Viral stocks were produced in H1- HeLa cells by transfection of *in vitro* transcribed RNAs as described previously (Maynell et al., 1992; Racaniello, 1984). Virus was diluted in PBS with 0.01% $CaCl_2$, 0.01% $MgCl_2$ and cell absorption was carried out for 30–45 min at 37 °C before addition of media. Stocks were titered by plaque assay on H1-HeLa cells or $TCID_{50}$ assay on 293T and WI-38 cells. 293T cells were transfected using Effectene (Invitrogen) according to manufacturer's instructions. Plasmid was first diluted 1:5 with empty vector to reduce expression levels. The GFP-LC3 plasmid has been described previously and is available from AddGene (www.addgene.org, plasmid 11546) (Jackson et al., 2005). Lentivirus plasmids were provided by Dr. Richard Mulligan (Mostoslavsky et al., 2006). Tamoxifen (Sigma) and rapamycin (LC Labs) were dissolved in a 1:1 solution of DMSO:EtOH. 3-methyladenine (Sigma) was dissolved directly into media.

Immunofluorescence

WI-38 cells grown on cover slips were infected at four logs above the $TCID_{50}$, fixed at room temperature (RT) for 10 min in 4% formaldehyde, and permeabilized in PBS-BT (PBS with 3% BSA, 0.1% Triton X-100) at RT for 15 min. Primary and secondary antibody incubations were for 30 min at RT, and cells were subjected to three washes with PBS-BT between antibody incubations. Mitochondria were labeled with MitoTracker (Molecular Probes) according to manufacturer's instructions. Antibody against Protein Disulphide Isomerase (PDI, Abcam) was used at dilutions of 1:100. Antibody

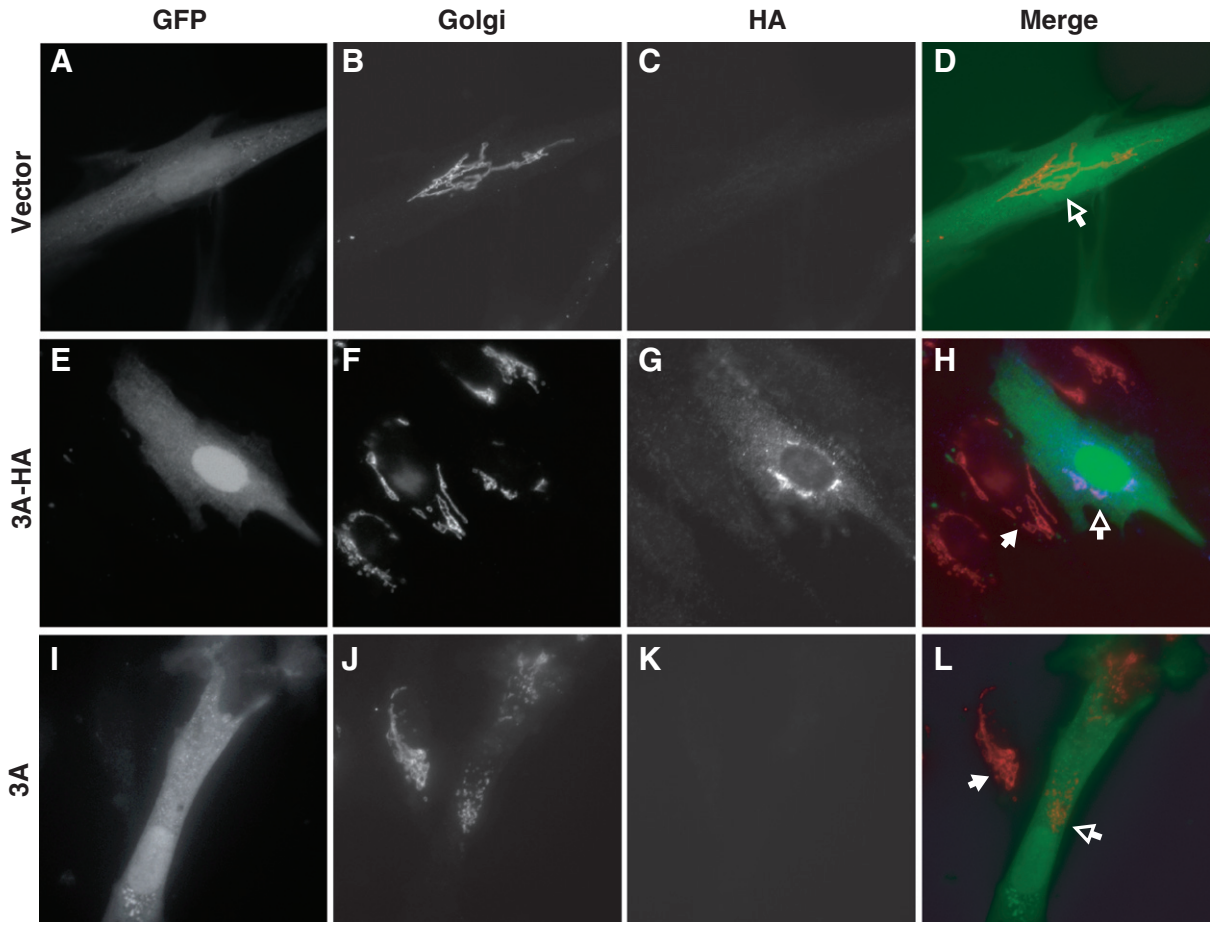

Fig. 8. Expression of HRV-1A 3A protein. Expression of 3A or 3A-HA proteins in the absence of HRV-1A infection. The lentivirus expression system used expresses GFP as a marker of infection. Protein expression was allowed to proceed for 72 h before cells were processed for immunofluorescence. Giantin (Golgi marker) was detected with Alexa Fluor 647 nm secondary antibody; HA tag was detected with Alexa Fluor 568 nm secondary antibody. Open arrowheads: cells which received lentivirus as indicated by GFP. Closed arrowheads: cells that did not receive lentivirus.

against Giantin (Covance) was used at 1:1000. Antibody against HRV-1A Capsid (ATCC) was used at 1:200. Appropriate Alexa Fluor-labeled secondary antibodies were used for visualization at dilutions of 1:250 (Molecular Probes). Coverslips were mounted with Vectashield (Vector Laboratories) and analyzed on a Nikon Eclipse TE2000-U microscope with MetaMorph software. Images were minimally processed in Adobe Photoshop 10.0.1.

Electron microscopy

WI-38 cells were placed in 10 cm dishes containing a coverslip. Cells were infected with HRV-1A at four logs above the $TCID_{50}$ for 24 h. Control cells were mock infected for 24 h. The coverslip was removed from each culture before fixation, placed in media, and cells were observed to confirm lysis at 48–54 h post-infection. Remaining cells were washed in 0.1 M Sörensens phosphate buffer adjusted to pH 7.4 + 0.05 mM CaCl. Fixation was performed in the dish with 1% glutaraldehyde + 4% paraformaldehyde in 0.1 M Sörensens buffer for 10 min. Cells were then washed in 0.1 M Sörensens buffer three times for 5 min each. Post fixation, cells were scraped from the plate, gently pelleted at 3000*g* for 5 min, and the pellets placed in freshly made reduced osmium tetroxide (1% OsO4 + 1.25% potassium haxacyanoferrate in distilled water 2 h on ice), dehydrated through graded methanol and processed into Embed 812 resin for EM observation of ultrathin (70 nm) sections. Cells were imaged on a JEOL 2100 or a Hitachi H600 microscope. For immunostaining, cell cultures were fixed in situ in a mixture of 4% paraformaldehyde and 0.1% glutaraldehyde in Sörensen's buffer on ice for 30 min. Following fixation the cells were washed (3 × 5 min) in buffer, scraped from the culture dishes, and gently pelleted at 2000G for 10 min. Cell pellets were processed into Lowicryl K4M resin using the progressively lower temperature (PLT) method of Berryman and Rodewald following the protocol of Burleigh et al. (Berryman and Rodewald, 1990; Burleigh et al., 1993). After UV polymerization, ultrathin (60 nm) sections were cut, mounted on formvar/carbon coated copper grids, and immuno-electron microscopy performed on the sections by incubating sequentially on 25 μl droplets in a humidified chamber. Anti-giantin was revealed using goat anti-rabbit 10 nm conjugated gold colloidal reagent (Electron Microscopy Sciences, Hatfield, PA). Double labeling was performed by first incubating with anti-GM130, revealed using goat anti-mouse 6 nM conjugated gold colloidal reagent, followed by 3 × 5-min washes in buffer then incubation with anti-Giantin, revealed by goat-anti rabbit 10 nM gold conjugate.

Fluorescent in situ hybridization

For hybridization experiments, cells were labeled with "Organelle Lights Golgi RFP" (Invitrogen) according to manufacturer's instructions. This induces expression of an RFP-tagged portion of N-acetylgalactosaminyltransferase-2, which localizes to Golgi stacks. After 48 h, cells were infected with HRV-1A. 24 h later cells were fixed and prepared for hybridization. Positive-stranded genomic RNA was produced from full-length HRV-1A cDNA using the Ambion MAXIscript kit in the presence of 488 nm labeled UTP (Molecular Probes). The transcription product was treated with DNAse, and unincorporated nucleotides were removed using Micro Bio Spin 6

columns (BioRad). The probes were subjected to alkaline hydrolysis for 90 min at 60 °C in 40 mM NAF3/60 mM Na2CO3, pH 10.2 to generate ~100 nt fragments (Cox et al., 1984). The hydrolysis reaction was stopped by addition of 0.1 M NaAc pH 6/0.5% glacial acetic acid, and probes were ethanol precipitated. Fragments greater than 100 nt were removed using a Micro Bio Spin 30 column. HRV-1A- and mock-infected WI-38 cells on cover slips were fixed and permeabilized for 10 min in 0.2%Triton X-100/4% formaldehyde. Following a PBS wash, aldehydes were quenched by adding PBS containing 0.5 M ammonium chloride for 7 min. Cover slips were placed in a moist chamber on top of 100 µl of hybridization buffer (5% formamide, 10 mM Tris HCl pH 7.4, 600 mM NaCl, 10% dextran sulfate, 10 mM DTT, 1% SDS, 200 µg/mL salmon sperm DNA) containing 100 ng of probe. Probes were allowed to hybridize at 40 °C for 40 h. Cells were then washed in 0.1× SSC [0.1 M NaCl, 0.015 M Sodium Citrate] at RT for 10 min, three times and imaged.

Lentivirus vector production and expression

The 3A protein of HRV-1A was PCR amplified, with or without the hemagglutanin (HA) tag sequence, and cloned into the lentivirus expression vector containing the cytomegalovirus (CMV) promoter and sequence for GFP (Mostoslavsky et al., 2006). Lentivirus particles were produced by transfecting five lentivirus-producing plasmids, including the expression plasmid, into 293T HEK cells at 30% confluency in a 10 cm dish, using TransIT-293 Transfection Reagent (Mirus, MIR 2700). Media from the transfected 293T cells was collected and replaced for three days. Supernatant was filtered through a .45u PVDF membrane to create a cell-free solution and was then centrifuged at 25,000 RPM for 2 h at 4 °C through a filter sterilized 20% sucrose solution [20 g ultrapure sucrose, 100 mM NaCl, 20 mM HEPES (pH 7.4) and 1 mM EDTA]. Virus pellet was resuspended in 100 µl of PBS and vortexed every 20 min for 2 h. Tubes were held at 4 °C in between vortexing, then removed. Remaining virus was washed from the ultracentrifuge tube in 150 µl of PBS and combined into 250 µl total virus stock. Virus was transferred onto PBS-washed WI-38 cells on coverslips. Lentivirus particles were absorbed into cells for 2 h at 37 °C, after which 1 mL of media was added to each well. The media was changed 48 h post-infection, and cells were processed for immunofluorescence upon observation of GFP expression, approximately 72 h post-infection. Imaging was performed on a Nikon Eclipse Ti microscope with Nikon Elements software.

Acknowledgments

We thank Clive Wells for electron microscopy and Richard Mulligan for providing lentivirus vectors. We acknowledge Charley Myers for invaluable advice on the care and feeding of BEAS-2B cells. We are grateful to Amy Hudson and Paula Traktman for experimental suggestions and support. We also thank Kathryn Klein, Alexsia Richards, and Kathleen Boyle for critical reading of the manuscript. C.A.Q. thanks S. D. for guidance. This work was supported by the Center for Infectious Disease Research and the Advancing a Healthier Wisconsin program.

Appendix A. Supplementary data

Supplementary data to this article can be found online at doi:10.1016/j.virol.2010.08.012.

References

Ait-Goughoulte, M., Kanda, T., Meyer, K., Ryerse, J.S., Ray, R.B., Ray, R., 2008. Hepatitis C virus genotype 1a growth and induction of autophagy. J. Virol. 82, 2241–2249.
Andries, K., Dewindt, B., Snoeks, J., Wouters, L., Moereels, H., Lewi, P.J., et al., 1990. Two groups of rhinoviruses revealed by a panel of antiviral compounds present sequence divergence and differential pathogenicity. J. Virol. 64, 1117–1123.
Belov, G.A., Altan-Bonnet, N., Kovtunovych, G., Jackson, C.L., Lippincott-Schwartz, J., Ehrenfeld, E., 2007. Hijacking components of the cellular secretory pathway for replication of poliovirus RNA. J. Virol. 81, 558–567.
Berryman, M.A., Rodewald, R.D., 1990. An enhanced method for post-embedding immunocytochemical staining which preserves cell membranes. J. Histochem. Cytochem. 38, 159–170.
Berstein, H.D., Baltimore, D., 1988. Poliovirus mutant that contains a cold-sensitive defect in viral RNA synthesis. J. Virol. 62, 2922–2928.
Beske, O., Reichelt, M., Taylor, M.P., Kirkegaard, K., Andino, R., 2007. Poliovirus infection blocks ERGIC-to-Golgi trafficking and induces microtubule-dependent disruption of the Golgi complex. J. Cell Sci. 120, 3207–3218.
Brabec-Zaruba, M., Berka, U., Blaas, D., Fuchs, R., 2007. Induction of autophagy does not affect human rhinovirus type 2 production. J. Virol. 81, 10815–10817.
Bui, Q.T., Golinelli-Cohen, M.P., Jackson, C.L., 2009. Large Arf1 guanine nucleotide exchange factors: evolution, domain structure, and roles in membrane trafficking and human disease. Mol. Genet. Genomics 282, 329–350.
Burleigh, B.A., Wells, C.W., Clarke, M.W., Gardinar, P.R., 1993. An integral membrane glycoprotein associated with an endocytic compartment of *Trypanosoma vivax*: identification and partial purification. J. Cell Biol. 120, 339–352.
Callahan, P.L., Mizutani, S., Colonno, R.J., 1985. Molecular cloning and complete sequence determination of RNA genome of human rhinovirus type 14. Proc. Natl. Acad. Sci. USA 82, 732–736.
Choe, S.S., Kirkegaard, K., 2004. Intracellular topology and epitope shielding of poliovirus 3A protein. J. Virol. 78, 5973–5982.
Cornell, C.T., Kiosses, W.B., Harkins, S., Whitton, J.L., 2006. Inhibition of protein trafficking by coxsackievirus b3: multiple viral proteins target a single organelle. J. Virol. 80, 6637–6647.
Cox, K.H., DeLeon, D.V., Angerer, L.M., Angerer, R.C., 1984. Detection of mrnas in sea urchin embryos by in situ hybridization using asymmetric RNA probes. Dev. Biol. 101, 485–502.
Doedens, J.R., Giddings Jr., T.H., Kirkegaard, K., 1997. Inhibition of endoplasmic reticulum-to-Golgi traffic by poliovirus protein 3A: genetic and ultrastructural analysis. J. Virol. 71, 9054–9064.
Dolan, T.M., Fenters, J.D., Fordyce, P.A., Holper, J.C., 1968. Rhinovirus plaque formation in WI-38 cells with methylcellulose overlay. Appl. Microbiol. 16, 1331–1336.
Dreux, M., Gastaminza, P., Wieland, S.F., Chisari, F.V., 2009. The autophagy machinery is required to initiate hepatitis C virus replication. Proc. Natl. Acad. Sci. USA 106, 14046–14051.
Duechler, M., Skern, T., Blaas, D., Berger, B., Sommergruber, W., Kuechler, E., 1989. Human rhinovirus serotype 2: in vitro synthesis of an infectious RNA. Virology 168, 159–161.
Fenters, J.D., Fordyce, P.A., Gerin, J.L., Holper, J.C., 1967. Propagation of rhinovirus on WI-38 cell monolayers in rolling bottles. Appl. Microbiol. 15, 1460–1464.
Gazina, E.V., Mackenzie, J.M., Gorrell, R.J., Anderson, D.A., 2002. Differential requirements for COPI coats in formation of replication complexes among three genera of picornaviridae. J. Virol. 76, 11113–11122.
Hamasaki, M., Noda, T., Ohsumi, Y., 2003. The early secretory pathway contributes to autophagy in yeast. Cell Struct. Funct. 28, 49–54.
Hidalgo, J., Garcia-Navarro, R., Gracia-Navarro, F., Perez-Vilar, J., Velasco, A., 1992. Presence of Golgi remnant membranes in the cytoplasm of brefeldin A-treated cells. Eur. J. Cell Biol. 58, 214–227.
Ishihara, N., Hamasaki, M., Yokota, S., Suzuki, K., Kamada, Y., Kihara, A., et al., 2001. Autophagosome requires specific early sec proteins for its formation and NSF/SNARE for vacuolar fusion. Mol. Biol. Cell 12, 3690–3702.
Jackson, W.T., Giddings Jr., T.H., Taylor, M.P., Mulinyawe, S., Rabinovitch, M., Kopito, R.R., et al., 2005. Subversion of cellular autophagosomal machinery by RNA viruses. PLoS Biol. 3, e156.
Khakpoor, A., Panyasrivanit, M., Wikan, N., Smith, D.R., 2009. A role for autophagolysosomes in dengue virus 3 production in HepG2 cells. J. Gen. Virol. 90, 1093–1103.
Kirkegaard, K., 1992. Genetic analysis of picornaviruses. Curr. Opin. Genet. Dev. 2, 64–70.
Kistler, A., Avila, P.C., Rouskin, S., Wang, D., Ward, T., Yagi, S., et al., 2007. Pan-viral screening of respiratory tract infections in adults with and without asthma reveals unexpected human coronavirus and human rhinovirus diversity. J. Infect. Dis. 196, 817–825.
Klionsky, D.J., Abeliovich, H., Agostinis, P., Agrawal, D.K., Aliev, G., Askew, D.S., et al., 2008. Guidelines for the use and interpretation of assays for monitoring autophagy in higher eukaryotes. Autophagy 4, 151–175.
Knoops, K., Kikkert, M., Worm, S.H., Zevenhoven-Dobbe, J.C., van der Meer, Y., Koster, A.J., et al., 2008. SARS-coronavirus replication is supported by a reticulovesicular network of modified endoplasmic reticulum. PLoS Biol. 6, e226.
Knox, C., Moffat, K., Ali, S., Ryan, M., Wileman, T., 2005. Foot-and-mouth disease virus replication sites form next to the nucleus and close to the Golgi apparatus, but exclude marker proteins associated with host membrane compartments. J. Gen. Virol. 86, 687–696.
Lama, J., Guinea, R., Martinez-Abarca, F., Carrasco, L., 1992. Cloning and inducible synthesis of poliovirus nonstructural proteins. Gene 117, 185–192.
Lee, Y.R., Lei, H.Y., Liu, M.T., Wang, J.R., Chen, S.H., Jiang-Shieh, Y.F., et al., 2008. Autophagic machinery activated by dengue virus enhances virus replication. Virology.
Lopez-Souza, N., Favoreto, S., Wong, H., Ward, T., Yagi, S., Schnurr, D., et al., 2009. In vitro susceptibility to rhinovirus infection is greater for bronchial than for nasal airway epithelial cells in human subjects. J. Allergy Clin. Immunol. 123, 1384-90.e2.
Maynell, L.A., Kirkegaard, K., Klymkowsky, M.W., 1992. Inhibition of poliovirus RNA synthesis by brefeldin A. J. Virol. 66, 1985–1994.
Miller, S., Krijnse-Locker, J., 2008. Modification of intracellular membrane structures for virus replication. Nat. Rev. Microbiol. 6, 363–374.

Miller, D.J., Schwartz, M.D., Ahlquist, P., 2001. Flock house virus RNA replicates on outer mitochondrial membranes in drosophila cells. J. Virol. 75, 11664–11676.
Moradpour, D., Gosert, R., Egger, D., Penin, F., Blum, H.E., Bienz, K., 2003. Membrane association of hepatitis C virus nonstructural proteins and identification of the membrane alteration that harbors the viral replication complex. Antivir. Res. 60, 103–109.
Mostoslavsky, G., Fabian, A.J., Rooney, S., Alt, F.W., Mulligan, R.C., 2006. Complete correction of murine artemis immunodeficiency by lentiviral vector-mediated gene transfer. Proc. Natl. Acad. Sci. USA 103, 16406–16411.
Palmenberg, A.C., Spiro, D., Kuzmickas, R., Wang, S., Djikeng, A., Rathe, J.A., et al., 2009. Sequencing and analyses of all known human rhinovirus genomes reveal structure and evolution. Science 324, 55–59.
Racaniello, V.R., 1984. Studying poliovirus with infectious cloned cDNA. Rev. Infect. Dis. 6 (Suppl 2), S514–S515.
Radulescu, A.E., Siddhanta, A., Shields, D., 2007. A role for clathrin in reassembly of the Golgi apparatus. Mol. Biol. Cell 18, 94–105.
Rust, R.C., Landmann, L., Gosert, R., Tang, B.L., Hong, W., Hauri, H.P., et al., 2001. Cellular COPII proteins are involved in production of the vesicles that form the poliovirus replication complex. J. Virol. 75, 9808–9818.
Salonen, A., Vasiljeva, L., Merits, A., Magden, J., Jokitalo, E., Kaariainen, L., 2003. Properly folded nonstructural polyprotein directs the Semliki forest virus replication complex to the endosomal compartment. J. Virol. 77, 1691–1702.
Sir, D., Liang, C., Chen, W.L., Jung, J.U., Ou, J.H., 2008. Perturbation of autophagic pathway by hepatitis C virus. Autophagy 4, 830–831.
Spuul, P., Salonen, A., Merits, A., Jokitalo, E., Kaariainen, L., Ahola, T., 2007. Role of the amphipathic peptide of Semliki forest virus replicase protein nsP1 in membrane association and virus replication. J. Virol. 81, 872–883.
Suhy, D.A., Giddings Jr., T.H., Kirkegaard, K., 2000. Remodeling the endoplasmic reticulum by poliovirus infection and by individual viral proteins: an autophagy-like origin for virus-induced vesicles. J. Virol. 74, 8953–8965.
Tan, T.T., Bhuvanakantham, R., Li, J., Howe, J., Ng, M.L., 2009. Tyrosine 78 of premembrane protein is essential for assembly of West Nile virus. J. Gen. Virol. 90, 1081–1092.
Tang, H., Grise, H., 2009. Cellular and molecular biology of HCV infection and hepatitis. Clin. Sci. (Lond.) 117, 49–65.
Tang, D., Mar, K., Warren, G., Wang, Y., 2008. Molecular mechanism of mitotic Golgi disassembly and reassembly revealed by a defined reconstitution assay. J. Biol. Chem. 283, 6085–6094.
Tanida, I., Minematsu-Ikeguchi, N., Ueno, T., Kominami, E., 2005. Lysosomal turnover, but not a cellular level, of endogenous LC3 is a marker for autophagy. Autophagy 1, 84–91.
Taylor, M.P., 2007. Utilization of autophagy protein LC3 during poliovirus infection. Ph.D. Thesis, Stanford University School of Medicine.
Taylor, M.P., Burgon, T.B., Kirkegaard, K., Jackson, W.T., 2009. Role of microtubules in extracellular release of poliovirus. J. Virol. 83, 6599–6609.
Teterina, N.L., Egger, D., Bienz, K., Brown, D.M., Semler, B.L., Ehrenfeld, E., 2001. Requirements for assembly of poliovirus replication complexes and negative-strand RNA synthesis. J. Virol. 75, 3841–3850.
Teterina, N.L., Rinaudo, M.S., Ehrenfeld, E., 2003. Strand-specific RNA synthesis defects in a poliovirus with a mutation in protein 3A. J. Virol. 77, 12679–12691.
Uncapher, C.R., DeWitt, C.M., Colonno, R.J., 1991. The major and minor group receptor families contain all but one human rhinovirus serotype. Virology 180, 814–817.
Wells, V.R., Plotch, S.J., DeStefano, J.J., 2001. Determination of the mutation rate of poliovirus RNA-dependent RNA polymerase. Virus Res. 74, 119–132.
Wessels, E., Duijsings, D., Lanke, K.H., van Dooren, S.H., Jackson, C.L., Melchers, W.J., et al., 2006. Effects of picornavirus 3A proteins on protein transport and GBF1-dependent COP-I recruitment. J. Virol. 80, 11852–11860.
Wong, J., Zhang, J., Si, X., Gao, G., Mao, I., McManus, B.M., et al., 2008. Autophagosome supports coxsackievirus B3 replication in host cells. J. Virol. 82, 9143–9153.